NASA Technical Memorandum 86898

NASA-TM-86898 19850007787

High Temperature Thermocouple and Heat Flux Gauge Using a Unique Thin Film-Hardware Hot Junction

Curt H. Liebert, Raymond Holanda,
Steven A. Hippensteele, and Charles A. Andracchio
Lewis Research Center
Cleveland, Ohio

December 1984

HIGH TEMPERATURE THERMOCOUPLE AND HEAT FLUX GAUGE USING A UNIQUE THIN FILM-HARDWARE HOT JUNCTION*

Curt H. Liebert, Raymond Holanda, Steven A. Hippensteele,
and Charles A. Andracchio
National Aeronautics and Space Administration
Lewis Research Center
Cleveland, Ohio 44135

SUMMARY

A special thin film-hardware material thermocouple (TC) and heat flux gauge concept for a reasonably high temperature and high heat flux flat plate heat transfer experiment was fabricated and tested to gauge temperatures of 911 K. This unique concept was developed for minimal disturbance of boundary layer temperature and flow over the plates and minimal disturbance of heat flux through the plates. Comparison of special heat flux gauge Stanton number output at steady-state conditions with benchmark literature data was good and agreement was within a calculated uncertainty of the measurement system. Also, good agreement of special TC and standard TC outputs was obtained and the results are encouraging. Oxidation of thin film thermoelements was a primary failure mode after about 5 hr of operation.

INTRODUCTION

Experimental verification of analytical predictions for local wall temperature and Stanton number (nondimensional heat transfer coefficient) is very difficult because there is a lack of instrumentation for obtaining accurate measurements at operating conditions (ref. 1). A basic difficulty is that the thermocouple (TC) temperature sensors and heat flux gauges for Stanton number measurement must be very small and nonintrusive. Measurements of metal temperature and Stanton number in zones of airfoil boundary layer separation, laminar-to-turbulent transition and relaminarization are especially important. The accumulation of reliable measurements at these boundary layer conditions is necessary for the assessment of dependable design tools for high temperature gas turbine engines.

The use of thin film materials to form TC's is not new. Reference 2 describes the use of thin film TC's for measurement of gun bore surface temperatures. Reference 3 describes early preliminary investigations of techniques for sputtering thin film TC's on turbine blade materials and aerodynamic surfaces. Thin film TC's are advantageous because they will minimally disturb the boundary layer temperature or flow over the blade or heat flux into the blade. Reference 3 demonstrated that thin film TC's could accurately record

---

*A shorter version of this report will be presented at the Thirtieth International Gas Turbine Conference sponsored by the American Society of Mechanical Engineers, Houston, Texas, March 17-21, 1985.

high steady-state metal temperatures to 1020 K with potential to higher temperatures. References 4 to 6 describe some recent efforts in the development of thin film surface TC's for measurement of air-cooled turbine blade temperatures.

References 7 and 8 discuss investigations of high temperature embedded wire TC heat flux gauges and embedded Gardon heat flux gauge sensors instrumented with wire TC's. These gauges were designed for use under one-dimensional heat flux conditions through the gauge. The embedded TC heat flux sensors were designed with single conductor swaged wires. Both an Alumel and Chromel wire were embedded in the cold side of the hardware and an Alumel wire was embedded in the hot side. The sensor output was obtained as a differential signal from the Alumel wires. The Chromel-Alumel TC produces a reference temperature. In the Gardon gauge concept, two Alumel wires and one Chromel wire were installed in sheaths to form small three-conductor cables. These wires were extended from the cable and were fastened in cavities machined into hardware cold-side surfaces. The cavities were filled with ceramic cement. One Alumel lead was attached to the bottom center of the cavity; the other Alumel and Chromel leads were attached to the wall of the cavity near the bottom. Differential signal output was obtained from the Alumel wires.

An investigation was initiated to create, fabricate, test, and analytically model a special high temperature thin film-hardware material measurement system and heat flux gauge concept which is different from those described in references 3 to 8. This concept incorporates the economical use of only one sputtering operation to form nonintrusive thermoelements. The concept involves sputtering an electrically insulating thin film coating over most of the hardware metal surface exposing only bare metal material at locations where metal temperature measurement is desired. Thin film thermoelement legs (nickel) of a metal material different from the hardware material are then sputtered simultaneously onto the bare metal locations, the electrically insulating coating and thin-film-to-leadwire connectors. Sputter deposition of the legs onto the bare-metal (SS316) hardware locations forms the unique TC hot junction. The hardware material serves as the other common thermoelement. Heat flux gauges are formed by placing two thin film-hardware hot junctions opposite each other on the hardware hot and cold surfaces. This concept was created for minimal disturbance of boundary layer temperature and flow or heat flux through the plate.

The investigation was done in several steps. First, an air-cooled control flat plate instrumented with small embedded reference wire TC's and heat flux gauge sensors was designed, built, and tested. This control plate was designed for operation at reasonably high heat flux to give maximum temperature gradients from the hot to cold surfaces and minimum lateral temperature gradients within these surfaces. The control plate was instrumented for measurement of temperature gradients in three dimensions because it is necessary to know how temperature gradients are related to each other throughout the plate. The accuracy of the reference heat flux gauge sensors was determined by comparing their Stanton number outputs with experimental benchmark quality Stanton number data given in references 9 and 10. In this way, the reference gauge output on the control flat plate was calibrated with the benchmark data.

Secondly, the air-cooled control plate design was utilized on a second and third flat plate instrumented with the special thin film-hardware TC's and heat flux gauges. These special TC's were installed so that both temperature and

Stanton number measurements could be made. Film thicknesses of 3 μm and 10 to 12 μm were used on the second and third flat plates, respectively. Ceramic connectors were fabricated for attachment of the thin film thermoelements to lead wire connectors. Embedded reference wire TC's of the same type used for instrumentation of the control plate were installed adjacent to the special TC's only on the hot surface.

The results include data of temperature versus millivolt output of the TC materials used in this study. Comparison of special TC and reference TC steady-state output on plates 2 and 3 are presented. Also, comparisons were made of special heat flux gauge steady-state Stanton number output on plates 2 and 3 with reference gauge output obtained on plate 1 and with benchmark literature data. The comparisons were made at gas-temperature to gas-side plate temperature ratios of 1.3 to 1.4 which corresponds to some cooled turbine engine applications. Thin film fabrication, electrical circuitry and the uncertainties associated with the measurement system are also discussed.

SYMBOLS

c_p specific heat of gas, cal/gr•K

f/a fuel-to-air-ratio

h heat transfer coefficient, $W/m^2 \cdot K$

k thermal conductivity of heat flux gauge, i.e., flat plate, W/m•K

L length of gauge, m

Pr Prandtl number

p_g pressure, N/m^2

q heat flux, W/m^2

R gas constant, 82.0568 $cm^3 \cdot atm/(gr\ mole \cdot K)$

Re_x gas Reynold's number based on distance from flat plate leading edge, $Ux\rho/\mu$

St Stanton number

T temperature, K

T_f film temperature, $T_f = (T_g + T_A)/2$, K

T_g gas temperature, K

T_m average of gas-side and coolant-side flat plate temperatures, K

t time, sec

U velocity of gas, m/sec

X distance from the leading edge, m

x space coordinate, m

ρ density, kg/m^3, p/RT_f

μ gas viscosity, $N \cdot sec/m^2$

Subscripts:

A gas-side surface, upper surface of flat plate or gauge

D coolant-side surface, lower surface of flat plate or gauge

HEAT TRANSFER ANALYSIS

Temperature Distribution

The term one-dimensional is applied to a heat transfer problem when heat flows in only one direction within a heat conducting body. Such a situation rarely exists precisely in real heat transfer problems, but a great number of problems of practical engineering importance may be approximated quite well by assuming a one-dimensional condition. The one-dimensional heat flow equation is:

$$q = k \frac{(T_A - T_D)}{L}, \frac{W}{m^2} \tag{1}$$

This equation relates the heat flux to the temperature differences, $(T_A - T_D)$ measured differentially through the gauges (plate). Thermal conductivity data of the stainless steel 316 (SS316) flat plate gauge material used herein as a function of temperature is given in reference 11 (in table no. 331, curve number 64). A least square fit through the k versus T curve gives,

$$k = 9.25 + 0.015T_m , \frac{W}{m \cdot K} \tag{2}$$

The heat flux value obtained from the gauge is related to the gas-side heat transfer coefficient and driving temperature difference between the hot gas and flat plate gas-side surface as,

$$q = h(T_g - T_A), \frac{W}{m^2} \tag{3}$$

A definition for Stanton number is,

$$St = \frac{h}{(\rho U c_p)} \tag{4}$$

Combining equations (1) and (3) with (4),

$$St_x = \frac{k}{L} \frac{(T_A - T_D)/(T_g - T_A)}{\rho U c_p} \tag{5}$$

where c_p was evaluated at the film temperature, T_f. The accuracy of the reference gauges was determined by comparison of values with a turbulent equation of heat transfer

$$St\ Pr^{0.4} = 0.0287\ Re_x^{-0.2} \tag{6}$$

Equation (6) correlated the experimental benchmark Stanton number data given in references 9 and 10 for zero pressure gradient airflow over a flat plate and low heat flux though the plate within about 0 to 10 percent at turbulence levels of 0 to 6 percent. Values for thermodynamic and transport properties were taken from reference 12.

APPARATUS AND PROCEDURE

Test Facility and Flat Plates

A detailed description of the facility is given in reference 13. Briefly, the facility (as sketched in figure 5 of reference 13) is comprised of inlet, combustor, transition, air-cooled test vane, and exit sections. An air-cooled flat plate test section (fig. 1) was inserted 61 cm behind the air-cooled vane test section and ahead of the exit section shown in reference 13. The vanes were removed from the vane test section. Aircooled flat plates were machined from SS316 material to length and width dimensions of 17.8 and 8.5 cm. Flat plate gas-side surfaces were carefully machined and polished. Plate thickness was nominally 0.43 cm. Except at bolt locations, coolant-side surfaces were thermally insulated from the apparatus to which it was bolted. This design aided in reducing heat transfer from the plates to the apparatus, which in turn, aided in maintaining approximately uniform steady-state hot and cold lateral surface temperatures. The high k values of SS316 also aided to give nearly uniform hot and cold lateral surface temperatures. Test section and plates were designed for constant pressure along the gas-side surface in the flow direction. Hot gas was generated by burning either methane fuel in a J-47 gas turbine combustor or by burning Jet-A fuel in a J-58 gas turbine combustor. Hot combustion gas flowed over the leading edge of the plates and along the upper surface of the plates. Cooling air entered a duct fastened to the bottom of the plates and then flowed out into the hot gas stream through a slot machined into the rear of the plates. The cooling air duct dimensions were 0.65 cm high, 5.2 cm wide, and 11.1 cm long. The position of the duct entrance was 1 cm upstream of the longitudinal station 1 (fig. 2).

The test facility was designed to establish a uniform free-stream gas velocity distribution in front of the leading edge of the plate. Unpublished measurements previously made with a hot wire probe at gas temperatures of 300 to 400 K verified the establishment of a reasonably uniform velocity distribution in the vicinity of the plate wall at the leading edge. It was assumed that this velocity distribution was also established at gas temperatures up to 1098 K which was the highest gas temperature generated by the J-58 gas turbine combustor. Inlet total gas temperature and pressure were measured with a moveable probe positioned in front of the plate and measurements could be made over a distance of 1.3 cm from the top of the plate to within 1.3 cm from the top of the wall.

The experiments were performed with three flat plates. The first flat plate was instrumented with Chromel-Alumel miniature wire thermocouples and a total pressure probe mounted at the rear of the plate. This plate was used to investigate the reliability of obtaining nearly one-dimensional steady-state temperature gradients and heat fluxes through the plate. This plate was also used as a control to which the outputs from the special TC's and heat flux gauges on the second and third plates were compared.

Figure 2 schematically shows TC hot junction locations on the three flat plates. Longitudinal TC stations were designated by numerals 1, 2, 3, 4 and transverse TC stations were given by letters A, B, C. Two static pressure taps mounted in the top surface of the three plates were used to monitor pressure gradients in the flow direction. A three dimensional array of wire TC's was formed only on the control flat plate. A minimal amount of wire TC's were used. This reduced inaccuracies due to slots and wire TC assemblies which will interfere with the heat transfer process. Embedded wire TC hot junctions were placed very close to the top surface at a 0.038 cm depth. One dimensional heat conduction calculations were employed to correct the absolute temperature output to a value corresponding to the surface temperature. The plate thickness was about 11 times the depth of the grooves to cause no serious problems with heat path distortion within the plate.

SS316 was chosen for the flat plate thermoelement material because it easily oxidizes when heated in the hot combustion gases. Therefore, this is a good material for economically studying effects of oxidation on thermoelectric output over short running times. Structural changes which might indicate damage or deterioration were monitored by testing the resistance of each TC circuit after the rig was shutdown and had cooled off. After all the tests were completed, the plates were removed from the hot gas tunnel and inspected. The inspection consisted of circuit component resistance measurements, visual inspection and microscopic examination.

Procedure for Determination of Thermoelectric Characteristics

Analytical models for predicting the effects of alloying elements on TC thermoelectric characteristics are ineffective and so it is still necessary to rely on experimental calibration for determination of such properties. Calibrations of millivolt output versus temperature for SS316 versus Alumel and for SS316 versus nickel ranging from 273 to 1273 K were made. The calibrations were based on procedures discussed in reference 14. The slope of the SS316 versus Alumel calibration curve was used to determine differential temperature measurements on plate 1. The SS316 versus nickel calibrations were needed for determination of absolute and differential temperatures on plates 2 and 3. Calibration data were obtained on wire materials in 100 K intervals in both ascending and descending temperature modes. The Chromel-Alumel TC's were not calibrated because their millivolt output versus temperature are already known to a high degree of accuracy.

Wire TC Assemblies

Miniature Chromel-Alumel two-wire sheathed TC assemblies with outside diameter of 0.025 cm were used. These TC's were commercially available and of standard grade. They passed all TC acceptance tests described in reference 14.

These tests included inquiries into integrity of the sheath, electrical resistance of the insulation, junction integrity and tests for spurious emf.

On the top surface only, the assemblies were placed in grooves cut into the plates. The thermoelements of each TC were welded together to form hot junctions and flattened into a thickness of 0.008 cm. Then the hot junctions were laser welded to the bottom of the slots. Sheathed assemblies were laid into the grooves and then the groove voids above the assemblies and hot junctions were filled with nichrome material. Cover plates were spot welded to the plate surface. The cover plates and welds were dressed down to the surface of the plate and polished. On the cold side, the assemblies were strapped to the surface and hot junctions were laser welded in place.

Thin Film Thermoelement Fabrication on the Second and Third Plates

The components of a completely fabricated thin film-plate material temperature and heat flux gage sensor system on a flat plate are shown in figure 3. Appendix A discusses each component of the thin film-plate material system with comments relating to the design and fabrication procedures giving in table I. Sputtering parameters are given in table II. As discussed in appendix A, the thin films minimally disturbed the flow and temperature of the boundary layer or heat flux through the boundary layer.

Electrical Circuitry

The electrical circuitry for the thin film-plate material TC's and reference wire TC's is presented in appendix B.

Test Conditions

The experiments were conducted at the experimental conditions given in table III and a real-time-data-acquisition system was used to collect the data. Tests were performed by setting the desired combustion gas temperature and pressure to an exit critical velocity ratio of 0.5 (Mach number = 0.46). Then the cooling air flow rate was varied in a step-wise manner from test-point to test-point to establish a range of plate temperatures. Cooling-air mass flows and temperatures ranged from 1.36×10^{-3} to 1.90×10^{-2} kg/sec and 296 to 337 K. All data were taken at steady-state conditions. Measurements were not continued at plate temperatures greater than 911 K because it was observed after shutdown that the leading edge of the plate was softening. Two fuels were used to cover the temperature range. The first flat plate was operated at lower temperatures with methane fuel and at higher temperatures with JET A fuel. The second flat plate was operated using only methane fuel and the third flat plate was run using both methane and JET A fuel.

MEASUREMENT UNCERTAINTY

The discussion in appendix C describes statistical analysis used in the comparison and correlation of temperature measurements. The discussion also describes numerical analysis made prior to the tests for determination of the reasons for the dispersion and extent of dispersion (experimental error) expected from the temperature, Stanton number, and Reynold's number data taken

on the flat plates. The dispersion was compared with experimental dispersion obtained herein and in the literature.

RESULTS AND DISCUSSION

Thermoelectric Characteristics

The temperature-millivolt outputs of SS316-nickel and SS316-Alumel thermoelements are presented in table IV. The results show that there is adequate millivolt output between the alloys so that meaningful temperature difference measurements in a direction normal to the hot and cold surfaces of plates 1, 2, and 3 can be obtained from an amplified differential electrical signal generated from either SS316-Alumel or SS316-nickel circuitry. Also there is adequate output between these alloys so that unamplified absolute temperatures can be measured. The results from table IV were used to convert millivolts to temperature difference and to absolute temperature.

Standard Wire TC's and Heat Flux Gages on Control Plate

One-dimensional heat transfer. - Temperature differences measured with differential electrical signals in a direction normal to the hot and cold surfaces of control plate number 1 increased with increasing coolant-air mass flow while temperature differences in the transverse and longitudinal directions, i.e., lateral directions on the top and bottom surfaces remained relatively small. Absolute temperatures and temperature gradients were evaluated during a run at a high gas temperature of 1098 K. During this run the cooling-air mass flow was 8.62×10^{-3} kg/sec, gas pressure was 5.7×10^{5} N/m^2, exit critical velocity ratio was 0.5 and cooling air temperature was 310 K. These conditions established values of $(T_g - T_A)$ equal to 280 to 305 K. At this experimental condition, temperature gradients measured in a direction normal to the plate hot and cold surfaces were 230 to 283 K/cm while lateral temperature gradients within the surfaces ranged from only 3.5 to 7.5 K/cm in the longitudinal direction and 0 to 6.4 K/cm in the transverse direction. These lateral temperature gradients (in all plates) were evaluated by subtracting absolute temperature values and are accurate ±3 K/cm. Absolute lateral temperature variations measured within the surfaces were small and were within the calculated experimental error discussed in appendix C. The heat flux, within experimental error, is highly one-dimensional in a direction normal to the hot and cold surfaces with 97 percent of the heat flux in the normal direction. Heat flux values of 4.8×10^{5} to 6.3×10^{5} W/m^2 were measured in the normal direction.

Normal and lateral temperature differences in the plate were also evaluated at values of $(T_g - T_A)$ equal to 160 K. Lower values of this temperature difference term were not considered because, as discussed in appendix C, calculations indicated that Stanton number data scatter would be unacceptably high at $(T_g - T_A)$ values less than 160 K. This large data scatter was also experimentally observed. In the case of $(T_g - T_A) = 160$ K, experimental temperature gradients normal to the plate surfaces were 165 to 230 K/cm and lateral gradients were 0.4 to 3.5 K/cm. Gas temperature was 922 K, cooling-air mass flow was 3.95×10^{-3} kg/sec and cooling-air temperature was 325 K. Heat fluxes in the normal direction of 3.2×10^{5} to 3.9×10^{5} W/m^2 were measured. Again it was found that the heat flux is highly one-dimensional in a direction normal to the plate surfaces with 98 percent of the heat flux in this direction.

Stanton and Reynold's numbers. - Comparison of the control plate Stanton numbers (fig. 4) and the benchmark data correlated with equation (6) shows acceptable agreement within 6 to 11 percent. This percent dispersion of the data about values obtained with equation (6) generally corresponds to that obtained in references 9 and 10 at all gas conditions with Pr = 0.71 (ref. 12). The reasons for the dispersion of the data are discussed in appendix C. The stainless steel 316 plate oxidized during the course of the experiment but within experimental error, the Stanton numbers were repeatable. Thus, within experimental error, oxidation of the plate had no observable effect on the differential temperature measurement through the SS316-Alumel circuit.

Special Thin Film-Plate Material TC's and Heat Flux Gauges

Comparison of special and standard TC output. - The investigation of the special TC's and heat flux gauges was carried out on plates 2 and 3 at the same test conditions and also at the same temperature differences of $(T_g - T_A)$, and at the same three-dimensional temperature gradient ranges investigated on the control flat plate. At longitudinal station 4 (fig. 2), metal temperature measurements made with special thin film-plate material TC's agreed well with reference wire TC measurements. This agreement is shown in figure 5 which presents a plot of the thin film-plate material TC output at station 4B versus standard wire TC output at station 4A for thin film thermoelement thicknesses of 3 μm and 10 to 12 μm. The deviation of the data points produced by the outputs from these TC's is within 4 percent from a line of perfect correlation. This small deviation corresponds to lower values in the range of uncertainty of 3.29 to 9.20 percent determined from the rms statistical analysis presented in appendix C, for the uncertainty expected in comparison of wire and special TC outputs. The population linear correlation coefficient calculated from these data for both film thicknesses was a satisfactory 0.995 ± 1 percent based on 99.73 percent of the data falling within the range.

Comparisons of standard and special TC output over the entire gas and plate temperature range could not be made at longitudinal stations 1 to 3 (fig. 2) because of nickel thermoelement failure after about 5 hr of TC testing on both the thinner and thicker films. However, comparisons could be made at these stations over a smaller temperature range at lower temperatures and at test times less than 5 hr. These comparisons produced values of regression coefficients identical to those obtained at longitudinal station 4.

Comparison of Stanton number with standard and benchmark data. - For comparative purposes, the Stanton number data obtained with the special gauges is plotted in figure 4 along with the control plate Stanton number data. The range of Reynold's number (about 1.8×10^6 to 2.3×10^6) over which the Stanton number was determined with the special gauges is smaller than the Reynold's number range corresponding to Stanton number values obtained on the control plate (Re about 0.8×10^5 to 2.3×10^6). The range is smaller because the special gauge measurements were obtained at only one longitudinal location, station 4B, corresponding to X = 11.6 cm, whereas the reference data were obtained at longitudinal stations 1A and 1C corresponding to X = 5.6 cm and stations 3A and 3C corresponding to X = 9.6 cm. Special heat flux gauge measurements obtained with the thin film-plate TC's were consistent with the reference gauge Stanton number data and agreed well with the benchmark data. Also, the agreement was within a calculated uncertainty of the measurement system. This demonstrates that this special gauge concept using nonintrusive thin film-flat plate hardware material TC's to form temperature sensors and heat flux gauges is a viable

system. This has been demonstrated at conditions where values of T_A subtracted from T_g values are greater than 160 K. As discussed in appendix C, this system would probably be viable over a greater range of $(T_g - T_A)$ if this temperature difference quantity could be measured differentially.

Effects of Products of Combustion on Nickel Film Thermoelements

The silicon nitride sputtered onto the surface of the second plate showed no signs of deterioration, but stress cracks were noted at the step formed by the sputtered silicon nitride and the flame-sprayed alumina materials. Some erosion of the nickel films on plate 2 was noted in the region of the thin-film-to-leadwire connection and at the step from the silicon nitride to the ceramic layer. At a plate temperature of 800 K, two circuits failed because of thermal stress cracks and four circuits were inoperable because of nickel film failure due to oxidation. Although temperature measurements were repeatable during the tests, electrical resistance measurements on the films increased during the tests. This suggests that the nickel films were becoming thinner because of oxidation and possibly erosion. These films failed after about 5 hr of testing and also before Stanton number data could be obtained.

The 10 to 12 μm thick thin film-plate material TC sensor system sputter-deposited onto plate number 3 is shown in figures 3 and 6 after removal from the test section. This system was much more durable. The silicon nitride insulating film showed negligible degradation with no significant thermal stress cracking. This suggests that the silicon nitride sputtering process was under better control on the third flat plate. Resistance measurements indicated no significant degradation after TC testing for 4.1 hr. The thicker films successfully withstood two thermal cycles involving two rig startups and shutdowns during the 4.1 hr of testing. However, after an additional 0.9 hr of testing at higher gas temperature, five thin film-plate material TC's failed (figs. 3 and 6) at stations 1B, 2B, and 3B (fig. 2) before Stanton number data at higher $(T_g - T_A)$ values could be obtained. The other three TC's continued to operate over the duration of the tests for a total operating time of 6.8 hr. Two of these three TC's were located at station 4 on the top and bottom surfaces. Stanton numbers were determined with these TC's.

It is believed that the life of thin film thermoelements can be extended by increasing their thickness, by use of protective coatings, or by the use of more oxidation resistant materials.

CONCLUSIONS

The most important conclusion obtained from the results of this investigation was that a special thermocouple and one-dimensional heat flux gauge concept using a thin film-hardware material junction is a viable approach for measurement of surface temperature and heat flux. The concept can be used to measure the convective heat transfer between a gas and a wall in a channel flow situation.

Oxidation of thin film nickel thermoelements was the primary failure mode. Films 10 to 12 μm thick operated for about 7 hr over a temperature range of 391 to 911 K. The life of thin film thermoelements can be extended by increasing their thickness, development of protective coatings or use of more oxidation resistant materials.

APPENDIX A - THIN FILM THERMOELEMENT FABRICATION

The components of a completely fabricated thin film-plate material TC and heat flux gauge sensor system on the second and third flat plates is shown in figure 3. The fabrication procedures presented in table I are now described.

Leadwires

Use of nickel thin film thermoelements requires nickel leadwires to bring the signal from the plate. The installation procedure for nickel leadwires embedded in a flame-sprayed ceramic is given in items 4 to 9 of table I. This installation was made on both the top and bottom surfaces.

Electrical Insulation and Hot Junctions

After the nickel leadwire installations were fabricated, a thin film of silicon nitride 7.5 μm thick was sputtered onto the SS316 plate material (items 12 to 15, table I), but not onto the flame-sprayed material securing the leadwires. This film electrically insulated the nickel-thin films from the metal plate. A narrow strip along the longitudinal axis in the center of the plate was left uncoated (fig. 3) on both the top and bottom surfaces. It was upon this strip that sputtered nickel-thin film SS316 plate hot junctions were formed. The area of the hot junction was 0.3 cm^2. Silicon nitride was sputtered using the parameters given in table II.

Nickel Thin Film Thermoelements and Thin-Film-to-Leadwire Connectors

Nickel thin films were sputter-deposited over the silicon nitride and over the leads of the nickel wire on both the top and bottom surfaces of the plates (items 16 to 17, table I). Nickel films 10 to 12 μm thick sputtered onto plate number 3 are shown in figure 3. The sputtering parameters are given in table II. Thin-film-to-leadwire connections were made when sputtered material penetrates through the porous flame-sprayed ceramic to contact the leadwires and make an electrical junction. Machined metal masks were used to form thin film legs onto the surface. The serpentine path of the thermoelement shown in figure 3 resulted from the necessity for routing the thin film leg around the grooved area reserved for a wire TC installation.

Effect of Thin Films on Boundary Layer Conditions

The thin films of silicon nitride and nickel minimally disturbed the conditions of boundary layer flow, boundary layer temperature or heat flux through the boundary layer. The narrow, uncoated strip along the longitudinal axis and the nickel films sputter-deposited on the uncoated strip formed discontinuities in the surface profile. However, calculations showed that the ratio of the height of the discontinuity to the viscous sublayer thickness was about 0.3. Thus the wall for all practical purposes was aerodynamically smooth for a turbulent boundary layer since the height of the discontinuity was much less than the thickness of the sublayer. Heat conduction calculations at given gas temperature indicated that film temperature was increased by only 0.02 percent and heat flux was decreased by only 0.1 to 0.3 percent due to use of the films.

APPENDIX B - CIRCUITRY

Electrical circuitry for the thin film-plate material TC's is presented in figure 7. This circuitry also provided differential electrical signals for measurement of the temperature difference term ($T_A - T_D$) in equation (5). Stainless steel 316 wire of the same nominal chemical composition as the flat plate was welded to one end of the plate (table I, item 18). The SS316 wire and nickel leadwires were routed to insulated copper extension wires located about 1.5 m from the rig. Leadwire-to-extension wire junctions were electrically insulated and wrapped with thermal insulation into a single bundle. Three Chromel-Alumel reference TC's were mounted within the thermal insulation to measure an average bundle temperature. The copper leads were then routed through the test cell and secured in an interconnect box. Interconnect leads were routed to individual channels of a multiplex analog-to-digital converter. As the multiplex converter scanned each channel, only one channel measuring absolute temperatures or differential temperatures was switched in and out of the circuit at a time. The differential electrical signals were small and thus a 50X gain low noise amplifier was required. All TC pairs from the interconnect box were shielded to ground.

APPENDIX C - MEASUREMENT UNCERTAINTY

THERMOCOUPLE OUTPUTS

Correlation

Thin film-plate material outputs measured on the top surfaces of the second and third flat plates were compared with standard wire TC outputs measured at locations adjacent to them (fig. 2) by using linear least square analysis to obtain sample correlation coefficients. Fisher's Z transformation theory (ref. 15) was applied to the temperature data to determine population correlation coefficients and also to determine the extent of dispersion of the population at a three-sigma or 99.73 percent confidence level. The results from the correlation are given in the Results and Discussion section of this report.

TC Output Dispersion

Additional information about the dispersion was determined by combining the uncertainty of appropriate elements of the system. Table V lists uncertainties for each element contributing to the measurement error under items A and B. Values of the elements were estimated from previous experience in operation of the rig. The elements thought to mainly contribute to the dispersion are TC calibration, thermal radiation, random fluctuations in gas temperature and pressure, plate surfaces not perfectly isothermal, oxidation of the flat plate material and oxidation of thin films in hot combustion gases. Table V also lists the summation equations (ref. 5) used in calculating the range of root-mean-square uncertainty or dispersion expected in comparison of reference wire and special TC outputs, item C, and also in calculating the root-mean-square uncertainty in comparison of wire TC outputs with each other, item D. The range of rms uncertainty in item C is 3.29 to 9.20 percent and in item D is 3.06 to 8.67 percent.

Range of Stanton Number Uncertainty

Values for the $(T_g - T_A)$ term in equation (5) were not measured using the potentially more accurate differential electrical signal method because the TC measuring gas temperature could not be fabricated from the same material as the TC's mounted on the plates. Instead, absolute values of T_g and T_A were measured and then T_A was subtracted from T_g. Materials for the hot gas temperature probe were platinum versus platinum-13 percent rhodium which can resist the hot, corrosive combustion gas environment. Chromel-Alumel reference TC's were used to measure plate temperature because they can be fabricated into miniature TC's (ref. 16) with outputs accurately known. The reference TC's were embedded in the plates and therefore were not directly exposed to the hot combustion gas. This aids in their longevity. The special thin film-plate material TC's were formed from nickel because its combination with SS316 material has a high millivoltage output. Also, nickel and SS316 readily oxidize for rapid observation of oxidation effects on thin film-hardware material absolute and differential TC output. If materials less susceptible to high temperature oxidation had been incorporated in this study, the experiments would have taken longer and therefore would have been more expensive.

A numerical computation was made for estimating the Stanton number (eq. (5)) dispersion when T_A is subtracted from T_g. Representative conditions given in table VI were used in equation (5) to evaluate the Stanton numbers at five base values of $(T_g - T_A)$ shown in table VII. Values for the spaces marked with an asterisk in table VI are variables which depend upon the various base values of $(T_g - T_A)$ chosen for this calculation. Uncertainties in c_p depend on reference temperature.

The calculation was done by first calculating a base value for Stanton number. To do this, a base value of $(T_g - T_A)$ is taken and then T_A is calculated since T_g is given (table VI). Then T_D is calculated from the representative condition (table VI) $(T_A + T_D)/2 = 700$ K. The heat flux may now be determined from equations (1) and (2) and the value of L given in table VI. Next, T_f, is calculated. The density is determined from the given pressure, f/a ratio, R (table VI) and T_f; c_p is evaluated from reference 12 using values for p, f/a, and T_f. The St_x is calculated using equation (5) by noting that $k(T_A - T_D)/L$ is the heat flux. A value for U is given in table VI.

Next, the dispersion of Stanton number was calculated at given base $(T_g - T_A)$. The highest values in the Stanton number dispersion range were calculated by using the highest numbers in the condition range column of table VI for k and T_A, and with the lowest values for T_D, L, ρ, U, c_p, and T_g. Alternatively, the lowest values of k and T_A and the highest values for L, ρ, U, c_p, T_g and T_D were used to calculate the lowest Stanton number. This calculation produces the largest and smallest values of Stanton number at given base $(T_g - T_A)$ for definition of the Stanton number dispersion range. The largest and smallest values of St are then subtracted from the St calculated at the base $(T_g - T_A)$ and then divided by the St corresponding to the base $(T_g - T_A)$. This quantity is multiplied by 100 to give the percent dispersion Stanton number range shown in the last column of table VII. The dispersion (uncertainty) is very large at small given base values of $(T_g - T_A)$ and decreases with increasing base $(T_g - T_A)$ values.

The experimental results also showed trends of decreasing Stanton number dispersion with increasing values of $(T_g - T_A)$ values. The experimental Stanton number data scatter was acceptable at experimental $(T_g - T_A)$ equal to or greater than 160 K where values of Stanton number (fig. 4) +11 percent to -6 percent about correlation equation (6) were measured. The data scatter at $(T_g - T_A)$ values less than 160 K was unacceptably greater than $\pm$30 percent about equation (6).

The large Stanton number dispersion at small given base values of $(T_g - T_A)$ (table VII) can be associated with subtracting T_A from T_g terms in equation (5) which are close in value and where an uncertainty is associated with each temperature term. For instance, at $(T_g - T_A) = 50$ K, since $T_g = 1000$ K, $T_A = 950$ K. Values of T_g are known with an uncertainty of $\pm$1 percent so that T_g is either 1010 or 990 K (table VI). The value of T_A is known to an uncertainty of $\pm$0.75 percent so that its value is either 957 or 943 K. The uncertainty in $(T_g - T_A)$ is thus considered as 1010 - 943 = 67 K (or 990 - 957 = 33 K) at the given base value of 50 K. So the uncertainty in $(T_g - T_A)$ alone in equation (5) at the given base value of 50 K is (50K-33K)100/50 K = 34 percent (or -34 percent). These percentages are much larger than those given for the uncertainty in the other parameters in table VI ($\pm$0 to 2 percent). Next, if a lower value of $(T_g - T_A) = 160$ K is

considered, T_g is still 1000 K but T_A is now 840 K. Again, T_g is either 1010 or 990 K. The value of T_A is still assumed known $\pm$0.75 percent so that it is either 846 or 834 K. Then $(T_g - T_A)$ is either 176 or 144 K. The present uncertainty is now $\pm$10 percent instead of $\pm$34 percent.

A calculation was also made assuming that the value of $(T_g - T_A)$ could be determined directly from a differential electrical signal measurement rather than from subtracting values of T_A from T_g which gives rise to the large uncertainties in the $(T_g - T_A)$ term discussed above. When making a differential electrical signal measurement, the base term $(T_g - T_A)$ is presumed known $\pm$1 percent at all given base $(T_g - T_A)$ values taken in table VII. This calculation suggested that the Stanton number uncertainty would be less than $\pm$4 to 7 percent over the given base $(T_g - T_A)$ range of 50 to 240 K. These percentages are much smaller than the +57 to +21 percent at $(T_g - T_A)$ = 50 and 300 K or -7 to -28 percent shown in table VII. This calculation therefore suggests that the differential signal measurement is more accurate.

REFERENCES

1. Liebert, C.H., Gaugler, R.E., and Gladden, H.J., "Measured and Calculated Wall Temperatures on Air-Cooled Turbine Vanes with Boundary Layer Transition," NASA TM 83030, 1983.

2. Bendersky, D., "Special Thermocouple for Measuring Transient Temperatures," Mechanical Engineering, Vol. 75, No. 2 Feb. 1953, pp. 117-121.

3. Liebert, C.H., Mazaris, G.A., and Brandhorst, H.W. Jr., "Turbine Blade Metal Temperature Measurement with a Sputtered Thin Film Chromel-Alumel Thermocouple," NASA TM-X-71844, 1975.

4. Grant, H.P., and Przybyszewski, J.S., "Thin Film Temperature Sensor," PWA-5526-31, Pratt and Whitney Aircraft, East Hartford, CT, 1980, (NASA CR-159782).

5. Grant, H.P., Przybyszewski, J.S.; and Claing, R.G., "Turbine Blade Temperature Measurement Using Thin Film Temperature Sensors," PWA-5604, Pratt and Whitney Aircraft, East Hartford, CT, 1981. (NASA CR-165201).

6. Grant, H.P., et al., "Thin Film Temperature Sensors Phase III," PWA-5708-26, Pratt and Whitney Aircraft, East Hartford, CT, 1982. (NASA CR-165476).

7. Atkinson, W.H., Strange, R.R., "Development of Advanced High Temperature Heat Flux Sensors," PWA-5723-27, Pratt and Whitney Aircraft, East Hartford, CT, 1982. (NASA CR-165618).

8. Atkinson, W.H., Cyr, M.A., and Strange, R.R., "Turbine Blade and Vane Heat Flux Sensor Development. Phase I," PWA-5914-21, Pratt and Whitney Aircraft, East Hartford, CT, 1984. (NASA CR-168297).

9. Blair, M.F., "Influence of Free-Stream Turbulence on Boundary Layer Transition in Favorable Pressure Gradients," Journal of Engineering for Power, Vol. 104, No. 4, Oct. 1982, pp. 743-750.

10. Kays, W.M., Convective Heat and Mass Transfer, Second Edition McGraw-Hill, New York, 1980.

11. Touloukian, Y.S., et al., Thermophysical Properties of Matter, Vol. 1, IFI/Plenum, New York, 1970.

12. Poferl, D.J., Svehla, R.A., Lewandowski, K.: "Thermodynamic and Transport Properties of Air and the Combustion Products of Natural Gas and of ASTM-A-1 Fuel with Air," NASA TN D-5452, 1969.

13. Calvert, H.F., et al., "Turbine Cooling Research Facility," NASA TM X-1927, 1970.

14. Holanda, R., "Analysis of Thermoelectric Properties of High-Temperature Complex Alloys of Nickel-Base, Iron-Base, and Cobalt-Base Groups," NASA TP-2278, 1984.

15. Spiegel, M.R., "Theory and Problems of Statistics," Schaum's Outline Series, McGraw-Hill Book Company, 1961.

16. Holanda, R., Glawe, G. and Krause, L., "Miniature Sheathed Thermocouples for Turbine Blade Temperature Measurement," NASA TN D-7671, 1974.

TABLE I - THIN FILM-FLAT PLATE FABRICATION PROCEDURE

1. Polish plate surfaces to about 0.15 μm finish.
2. Drill and tap holes for coolant duct and mounting bracket
3 Drill holes for pressure taps, cut grooves for reference thermocouples, drill holes to pass wires from hot-gas side to cold-gas side of plate, cement insulators in holes to pass bare nickel wires through plate.
4 Grit-blast areas of plate designated for flame-sprayed material
5 Apply oxygen-acetylene flame-sprayed bond coat of nickel aluminum composite to areas designated for flame-sprayed material
6. Apply Rokide HiTec HT rod flame-sprayed insulating material base coat to a thickness of about 0 15 mm
7 Tape lead-wires in place.
8 Apply Rokide flame-sprayed material to leadwire pattern to a thickness of about 0 08 mm
9. Remove tape and apply Rokide flame-sprayed material to leadwire pattern to a thickness of about 0 03 mm.
10 Install reference thermocouples
11 Weld pressure taps to plate
12 Grit-blast surfaces for sputtering with 25 μm aluminum oxide grit at a pressure of 25 psi
13. Clean surfaces for sputtering with detergent, water, and alcohol
14 Mask plate and sputter first side of plate with silicon nitride to a thickness of 7 5 μm
15 Clean and mask plate and sputter second side of plate with silicon nitride to a thickness of 7.5 μm
16. Clean and mask plate and sputter first side of plate with nickel films to a thickness of 3 μm on plate 2 and 10 to 12 μm on plate 3
17. Clean and mask plate and sputter second side of plates with nickel films to same thickness
18. Weld stainless steel wire to plate

TABLE II. - SPUTTERING PARAMETERS

Sputtering material	Sputtering gas	Pressure, mtorr	Power, kW	Target-substrate distance, cm	Sputtering rate, μm/hr
Nickel	Argon	10	1.5	7 5	3
Silicon-Nitride	Argon plus Nitrogen	15	1 5	7.5	1.5

TABLE III - EXPERIMENTAL CONDITIONS FOR TESTS OF WIRE THERMOCOUPLES AND NICKEL THIN FILM/STAINLESS STEEL 316 FLAT PLATE THERMOCOUPLES

Plate no	Cooling-air temperature, K	Gas temperature, K	Burner type	Gas pressure, N/m^2	Film thickness	Range of plate temperatures, K		Duration of tests, hr	Plate no / test no
						Top	Bottom		
1	311	533	Nat gas	3.5×10^5	----	424-519	391-517	1.28	1/1 (wire TC)
	329	750	↓	5.7×10^5	----	530-657	475-646	2.67	1/2
	332	811		↓		614-736	569-719	——	——
	337	880				653-789	604-770	——	——
	320	672	ASTM-A-1	5.7×10^5		526-653	470-639	2.35	1/3
	310	1089	↓	↓		765-947	707-892	——	——
	325	922				669-879	586-879	——	——
2	296	533	Nat gas	3.1×10^5	3 μm	431-495	400-482	2.03	2/1 (thin film-s.s TC)
	302	672	↓	5.7×10^5	↓	541-621	497-608	——	——
	301	672		5.7×10^5		550-577	492-542	2.72	2/2
	307	811		↓		644-739	573-697	——	——
	313	880				694-794	606-685	——	——
3	287	537		3.1×10^5	10-12 μm	448-521	427-518	1.62	3/1 (thin film-s s TC)
	302	677		5.7×10^5	↓	551-626	500-627	——	——
	308	875	↓	5.7×10^5		682-786	631-769	——	——
	297	677	ASTM-A-1	5.7×10^5		549-580	509-554	2.08	3/2
	298	812	↓	↓		639-683	579-650	——	——
	296	879				651-694	572-658	——	——
	302	924		5.7×10^5		672-724	600-694	3.03	3/3
	302	980		↓		614-777	614-711	——	——
	301	1033				750-822	644-739	——	——
	304	1089	↓	↓	↓	911-753	874-672	——	——

TABLE IV - TEMPERATURE-MILLIVOLT CHARACTERISTICS FOR SS316-NICKEL AND SS316-ALUMEL THERMOCOUPLES USED HEREIN

Temperature, K	SS316-Ni, mV	SS316-Al, mV
273	0	0
323	----	0.88
373	1.94	1.76
423	----	2.55
473	4.15	-----
665	----	3.28
523	----	4.00
573	6.28	4.79
623	----	5.60
673	7.78	6.44
723	----	7.34
773	9.19	8.29
823	----	9.29
873	10.85	10.34
923	----	11.44
973	12.85	12.61
1023	----	13.81
1073	15.16	15.04
1123	----	16.32
1173	17.77	17.64
1273	20.67	-----

TABLE V. - TEMPERATURE MEASUREMENT UNCERTAINTIES OR EXPERIMENTAL ERROR EXPECTED IN COMPARISON OF VARIOUS THERMOCOUPLE OUTPUTS[a]

	Estimated uncertainty of i^{th} element, $\pm$ percent
A. Chromel-Alumel standard wire thermocouples-elements, A_i, contributing to measurement error	
1. Thermocouple calibration	0.75
2. Escort system	0.25
3. Thermal radiation	0.25 - 1.0
4. Random gas temperature fluctuations	1.0 - 3.0
5 Random gas pressure fluctuations	1 0 - 3 0
6. Plate surfaces not perfectly isothermal	1.0 - 3.0
7. Oxidation of flat plate material (could effect differential temperature measurement) in products of combustion	1.0 - 3.0
$\sum A_i^2$	4 69 - 37.63
B. Special thin film-flat plate material thermocouples-elements, B_i, contributing to measurement error	
1. Thermocouple calibration	1.00
2. Escort system	0.25
3. Thermal radiation	0 25 - 1.0
4 Random gas temperature fluctuations	1.0 - 3.0
5. Random gas pressure fluctuations	1.0 - 3 0
6. Plate surfaces not perfectly isothermal	1.0 - 3.0
7. Oxidation of flat plate material (could effect differential temperature measurement) in products of combustion	1.0 - 3.0
8. Oxidation of thin films in hot combustion gases	1 0 - 3.0
$\sum B_i^2$	6.13 - 47.06
C. Expected root-mean-square uncertainty in comparison of wire and special thermocouple outputs generated in either the top surface or the bottom surface of the flat plate	
$\left(\sum A_i^2 + B_i^2\right)^{1/2}$	3.29 - 9.20
D. Expected root-mean-square uncertainty in comparison of wire thermocouple outputs with each other generated in either the top surface or the bottom surface of the flat plate	
$\left(\sum A_i^2 + A_i^2\right)^{1/2}$	3.06 - 8.67

[a]Comparison made at the interface between the hot gas temperature and the top surface of the plate

TABLE VI. - REPRESENTATIVE CONDITIONS

	Condition (± uncertainty percent)	Condition range,[a]
L, m	4.57×10^{-2}(0.5)	4.59×10^{-2} to 4.55×10^{-2}
T_g, K	1000(1.0)	1010 to 990
k_b, W/m•K	20.25(2.0)	20.66 to 19.85
Average gauge temperature, $(T_A + T_D)/2$	700 K(0.7)	705 to 695
T_A	(c)(0.75)	(c)
T_D	(d)	(c)
f/a	0 010(0.5)	0.01
p, N	5.723×10^{5}(1.0)	5.78×10^{5} to 5.67×10^{5}
U, m/sec	289.6(1 0)	292 to 287
R, cm^3 atm/g mole, K	82.0568(0)	82.06

[a]Base condition times percent uncertainty.
[b]Evaluated at average gauge temperature.
[c]Values depend on given base values for $(T_g - T_A)$, table VII.
[d]Equals 0 75 for standard thermocouples and 1.0 for special thermocouples.

TABLE VII. - STANTON NUMBER DISPERSION

Given base temperature $(T_g - T_A)$, K	Base Stanton number calculated at base conditions and base temperature	Stanton number dispersion range	Percent Stanton number dispersion about base Stanton number
50	6.69×10^{-2}	1.05×10^{-1} to 4.8×10^{-2}	+57 to -28
100	2.56×10^{-2}	3.23×10^{-2} to 2.17×10^{-2}	+26 to -15
160	1.08×10^{-2}	1.27×10^{-2} to 9.74×10^{-3}	+18 to -9.8
240	2.93×10^{-3}	3.55×10^{-3} to 2.72×10^{-3}	+21 to -7.0
300	0	----------	----------

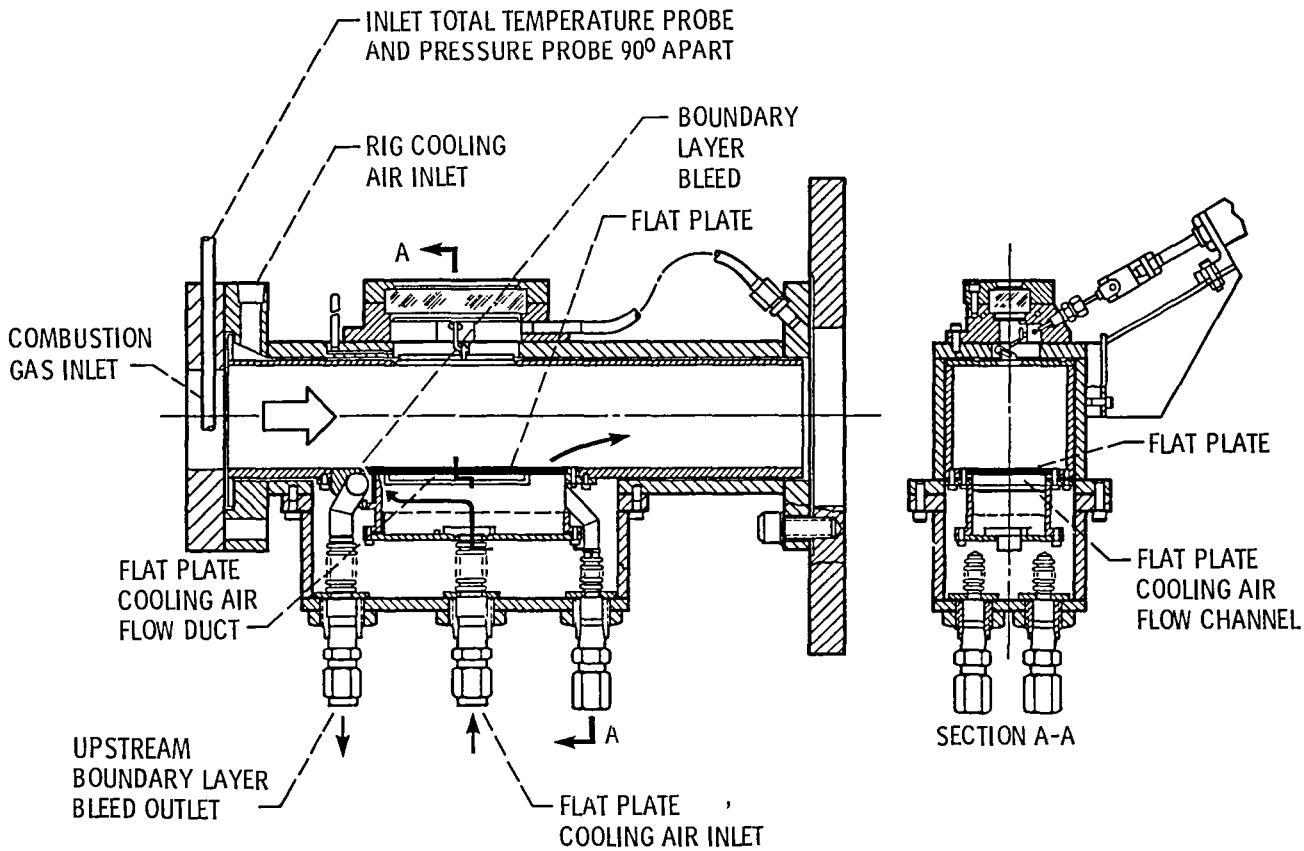

Figure 1. - Air cooled flat plate test section.

△ STATIC PRESSURE TAPS
○ EMBEDDED REFERENCE CHROMEL-ALUMEL WIRE THERMOCOUPLE HOT JUNCTION LOCATIONS IN CONTROL FLAT PLATE NUMBER 1
+ EMBEDDED REFERENCE CHROMEL-ALUMEL WIRE THERMOCOUPLE HOT JUNCTION LOCATIONS IN PLATES NUMBERED 2 AND 3
□ SPECIAL SPUTTERED THIN FILM-PLATE MATERIAL THERMOCOUPLE HOT JUNCTION LOCATIONS ON FLAT PLATES 2 AND 3

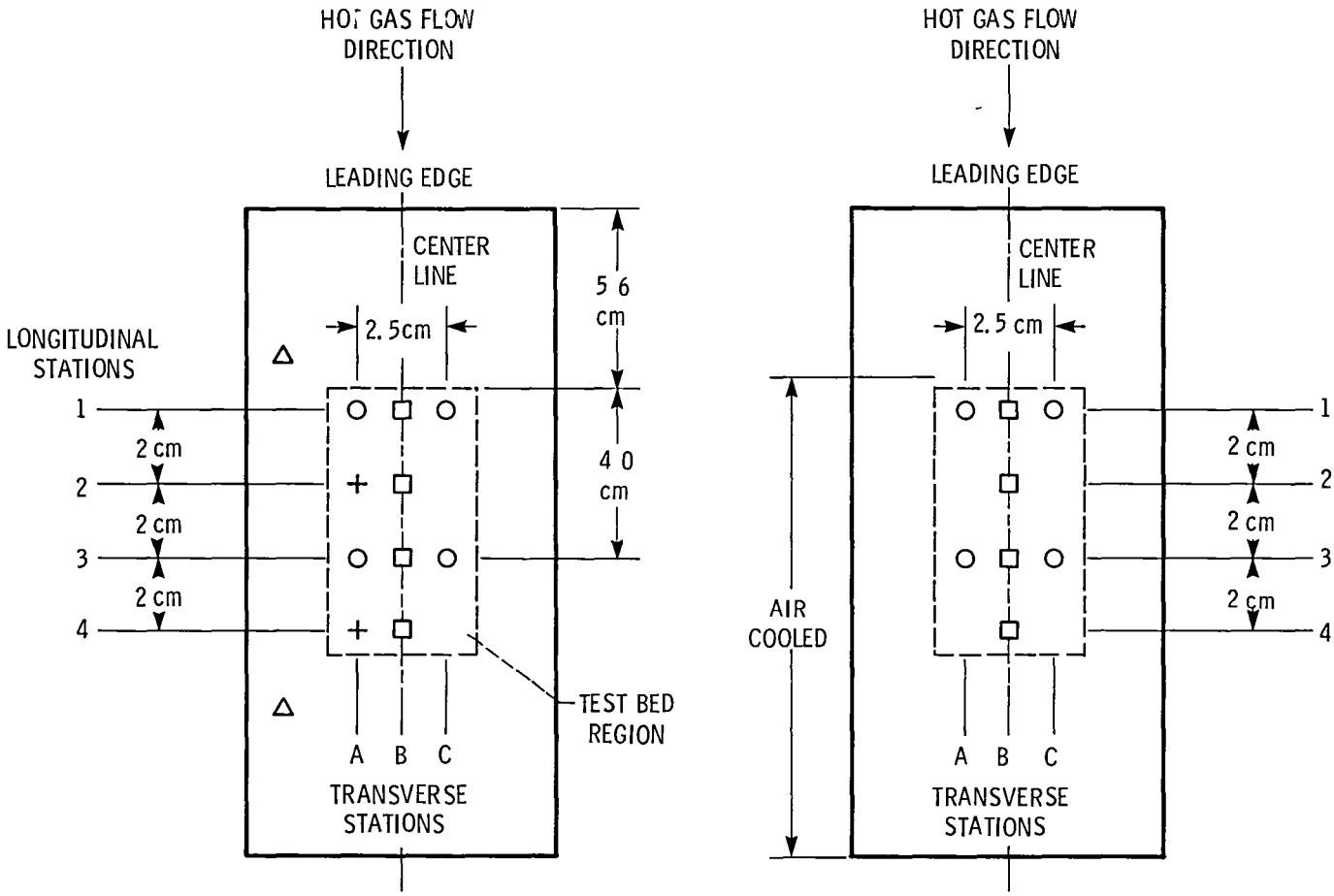

(a) Top-gas side surface

(b) Bottom-coolant side surface.

Figure 2. - Hot junction locations on flat plates.

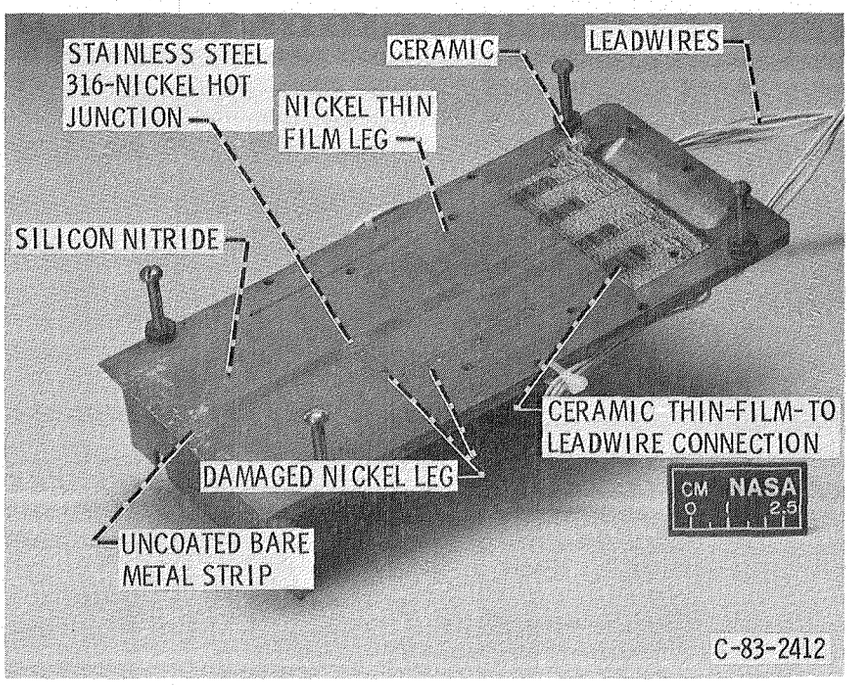

Figure 3. - View of flat plate hot side after tests with 10-12 micrometer thin film-plate material thermocouples.

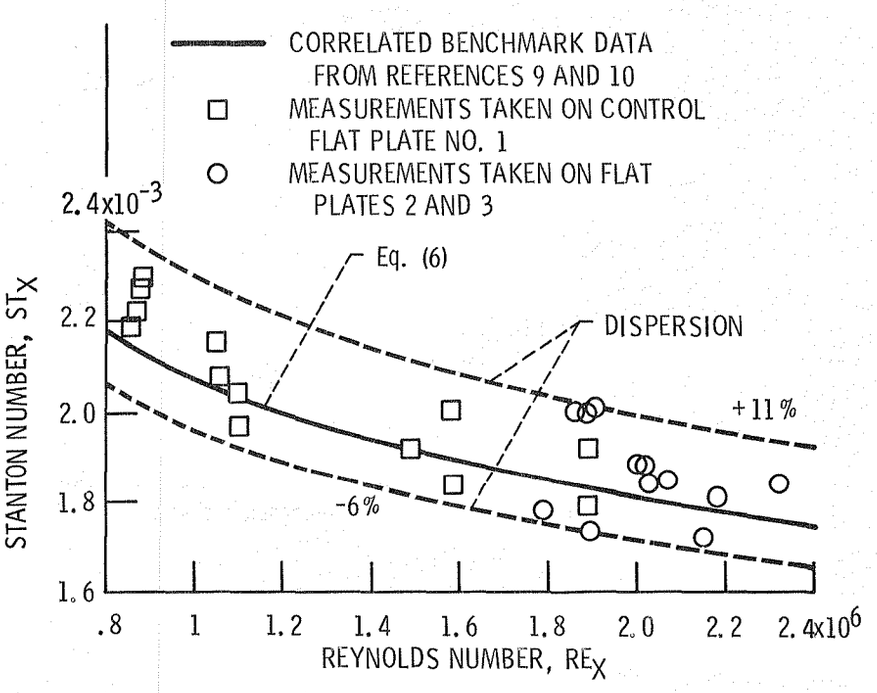

Figure 4. - Heat flux gage output at $(T_g - T_A)$ values greater than 160K.

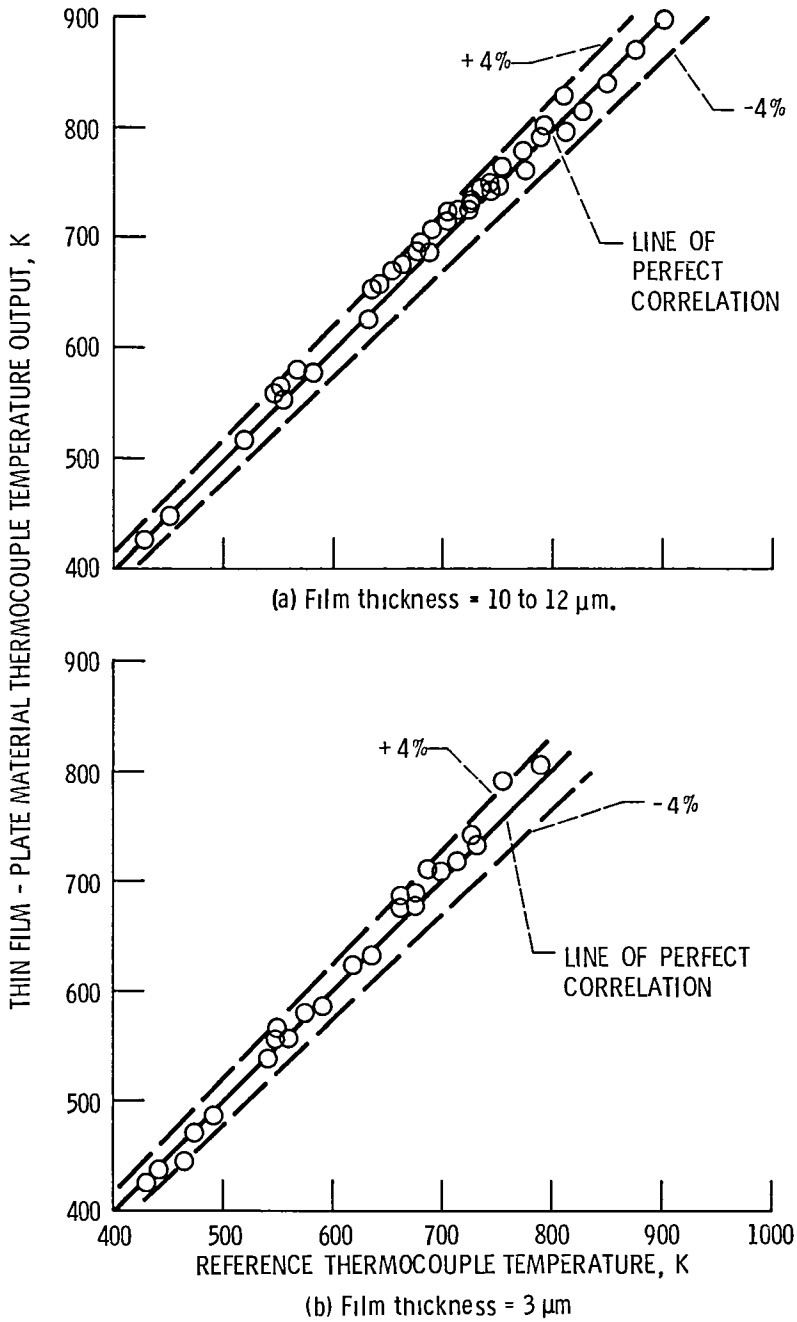

Figure 5. - Comparison of thin film - plate material thermocouple and standard thermocouple outputs at station 4A and 4B.

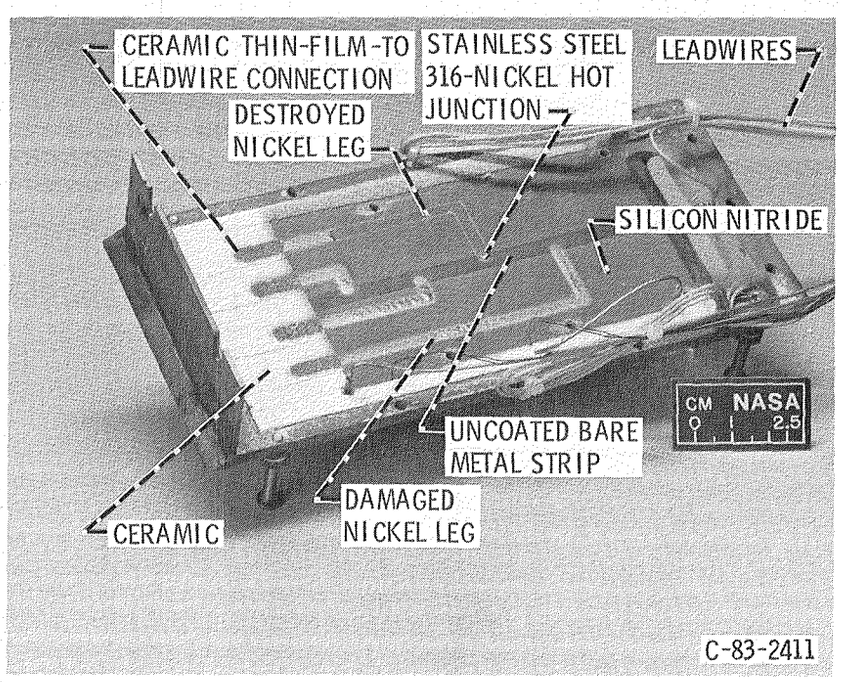

Figure 6. - View of cold side after tests with 10-12 micrometer thin film-plate material thermocouples.

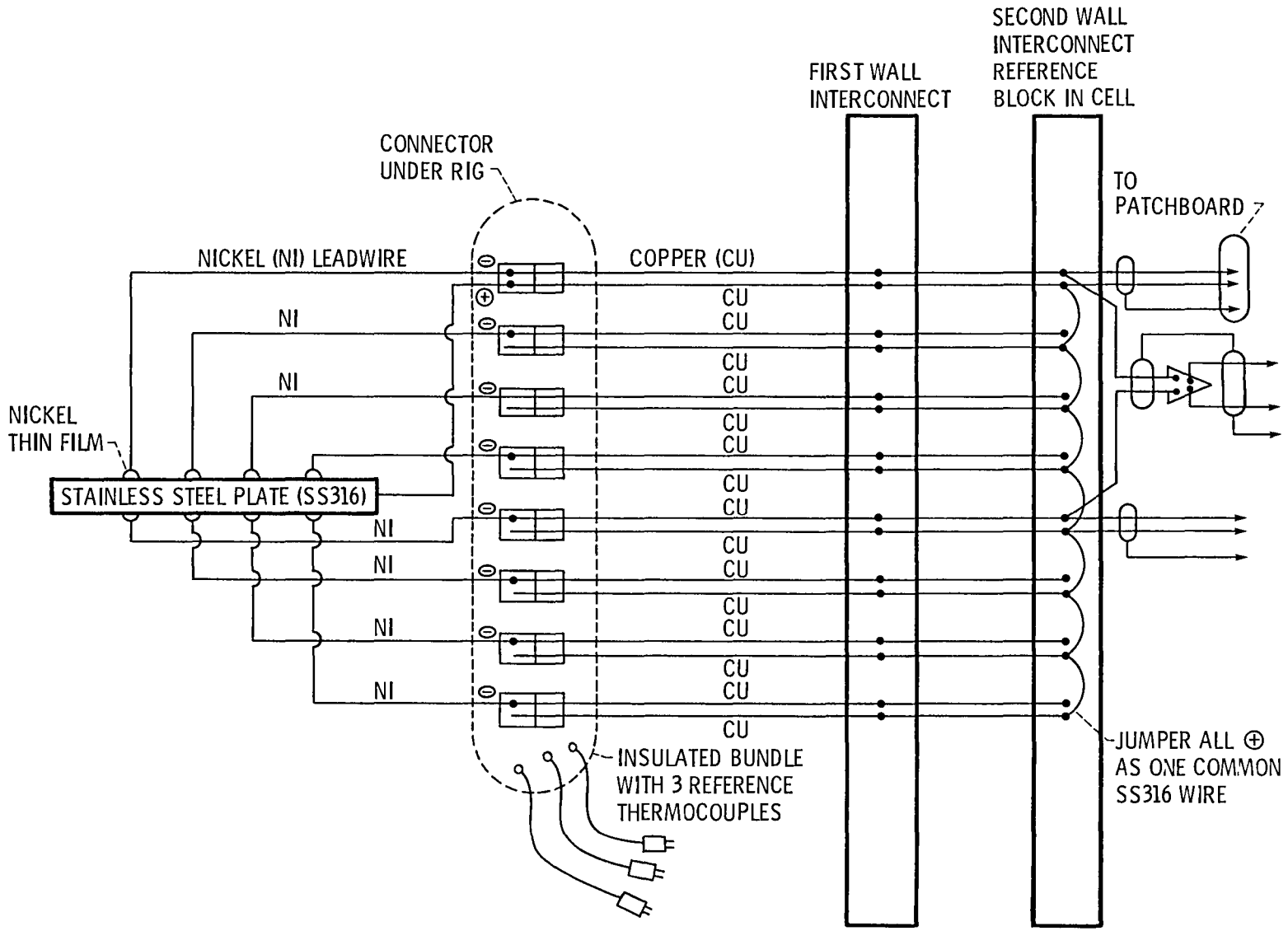

Figure 7. - Thin film-flat plate material thermocouple circuitry.

1 Report No	2 Government Accession No	3 Recipient's Catalog No
NASA TM-86898		

4 Title and Subtitle	5 Report Date
High Temperature Thermocouple and Heat Flux Gauge Using a Unique Thin Film-Hardware Hot Junction	December 1984
	6 Performing Organization Code: 533-04-1A

7 Author(s)	8 Performing Organization Report No
Curt H. Liebert, Raymond Holanda, Steven A. Hippensteele, and Charles A. Andracchio	E-2365
	10 Work Unit No

9 Performing Organization Name and Address	11 Contract or Grant No
National Aeronautics and Space Administration Lewis Research Center Cleveland, Ohio 44135	
	13 Type of Report and Period Covered: Technical Memorandum

12 Sponsoring Agency Name and Address	14 Sponsoring Agency Code
National Aeronautics and Space Administration Washington, D.C. 20546	

15 Supplementary Notes

A shorter version of this report will be presented at the Thirtieth International Gas Turbine Conference and Exhibit sponsored by the American Society of Mechanical Engineers, Houston, Texas, March 17-21, 1985.

16 Abstract

A special thin film-hardware material thermocouple (TC) and heat flux gauge concept for a reasonably high temperature and high heat flux flat plate heat transfer experiment was fabricated and tested to gauge temperatures of 911 K. This unique concept was developed for minimal disturbance of boundary layer temperature and flow over the plates and minimal disturbance of heat flux through the plates. Comparison of special heat flux gauge Stanton number output at steady-state conditions with benchmark literature data was good and agreement was within a calculated uncertainty of the measurement system. Also, good agreement of special TC and standard TC outputs was obtained and the results are encouraging. Oxidation of thin film thermoelements was a primary failure mode after about 5 hr of operation.

17 Key Words (Suggested by Author(s))	18 Distribution Statement
Thin films Thermocouple Heat flux gauges	Unclassified - unlimited STAR Category 35

19 Security Classif (of this report)	20 Security Classif (of this page)	21 No of pages	22 Price*
Unclassified	Unclassified		

*For sale by the National Technical Information Service, Springfield, Virginia 22161

End of Document